Available online at www.sciencedirect.com
ScienceDirect
Ocean Engineering 34 (2007) 2385–2399
OCEAN ENGINEERING
www.elsevier.com/locate/oceaneng

Optimal localization of a seafloor transponder in shallow water using acoustic ranging and GPS observations

Hsin-Hung Chen*, Chau-Chang Wang

Institute of Undersea Technology and Asian Pacific Ocean Research Center, National Sun Yat-sen University, Kaohsiung, Taiwan 804, ROC

Received 20 November 2006; accepted 15 May 2007
Available online 21 May 2007

Abstract

This study utilized circular and straight-line survey patterns for acoustic ranging to determine the position of a seafloor transponder and mean sound speed of the water column. To reduce the considerable computational burden and eliminate the risk of arriving at a local minimum on least-squares inversion, the position of a seafloor transponder was estimated by utilizing optimization approaches. Based on the implicit function theorem, the Jacobian for this inverse problem was derived to investigate the constraints of employing circular and straight-line survey patterns to estimate the position of a transponder. Both cases, with and without knowledge of the vertical sound speed profile, were considered. A transponder positioning experiment was conducted at sea to collect acoustic and GPS observations. With significant uncertainties inherent in GPS measurements and the use of a commercial acoustic transponder not designed for precise ranging, experimental results indicate that the transponder position can be estimated accurately on the order of decimeters. Moreover, the mean sound speed of the water column estimated by the proposed optimization scheme is in agreement with that derived from conductivity, temperature, and density (CTD) measurements.

Keywords: Transponder; Acoustic ranging; GPS; Sound speed; Circular survey; Straight-line survey; Localization; Optimization

1. Introduction

Since the 1970s, acoustic time-of-flight navigation systems, such as long baseline (LBL) and ultra-short baseline (USBL), have been employed in oceanographic instruments and vehicles (Milne, 1983; Caiti et al., 2005). A LBL system has an array of acoustic transponders deployed on the seafloor. The absolute location of a fixed seafloor transponder is first estimated from observations of acoustic ranges and GPS positions. Then, vehicles or oceanographic instruments can be tracked based on measurements of round trip travel ranges between seafloor transponders and an onboard transceiver. For USBL positioning, although a seafloor transponder is not needed, recent studies have shown that range and bearing measurements based on a known fixed seafloor transponder improve USBL positioning accuracy (Opderbecke, 1997; Philips, 2003).

The absolute position of a fixed transponder is usually estimated by the least-squares inversion based on acoustic and GPS observations (Shiobara et al., 1997; Yoerger et al., 2000; Osler and Beer, 2000; Kussat et al., 2005). However, one shortcoming of least-squares inversion is the significant computational burden incurred by accumulation of several hundred observations (Sweeney et al., 2005). Another shortcoming is that the nonlinear least-squares procedure can fall into local minima in the solution space. To estimate the position of a seafloor transponder, this study utilizes optimization approaches. This scheme facilitates the use of global optimization methods, such as genetic algorithms, to obtain the global minimum without a good initial guess. Additionally, the survey pattern used to collect observations is critical to the success

*Corresponding author. Tel.: +886 7 5252000x5282; fax: +886 7 5255270.
E-mail address: hhchen@mail.nsysu.edu.tw (H.-H. Chen).

0029-8018/$ - see front matter © 2007 Elsevier Ltd. All rights reserved.
doi:10.1016/j.oceaneng.2007.05.005

of localizing a seafloor transponder (Shevenell, 1984; Shiobara et al., 1997). Often, when estimating the position of a seafloor transponder, acoustic and GPS observations are collected by utilizing a straight-line survey pattern (Obana et al., 2000; Yamada et al., 2002) or circular survey pattern (Osada et al., 2003; Kussat et al., 2005). In fact, an improper survey path yields either non-unique solutions or false solutions which never converge; however, few studies have mentioned the feasibility of survey patterns on the inverse problem solution. In this study, the implicit function theorem (Hildebrand, 1976) is used to investigate constraints on circular and straight-line surveys for acquiring a unique solution.

Precise acoustic ranging requires accurate travel time measurement and knowledge of sound speed along the acoustic path. At present, travel time resolution of a few microseconds is possible (Sweeney et al., 2005), meaning that slant range measurement can be accurate to centimeters when sound speed is known. However, surveys generally last for hours when gathering a sufficient number of observations for estimating transponder position. Measuring sound speed profiles frequently during data collection is inappropriate as this is very time consuming. Since sound speed profiles of the water column are temporarily and spatially varied in the upper ocean, a small number of measured sound speed profiles cannot exactly represent the sound speed field through which the acoustic ray traveled. That is, the position estimate of a transponder is subject to errors due to spatial-temporal variations of sound speed. Additionally, ray-tracing calculations are typically performed when estimating the position of a transponder; however, this process is complex and time-consuming. Yamada et al. (2002) employed simulations to estimate the horizontal position of a transponder located on the seafloor at a depth of 1500 m. The sum of squared travel-time residuals was assessed by assuming that sound speed is uniform throughout the ocean. Yamada et al. located the seafloor transponder with only an 18-cm discrepancy. This simulation result indicates that it is possible to estimate the transponder position accurately within centimeters by assuming sound speed is uniform throughout the water column. Therefore, this study treats mean sound speed as an unknown parameter, which is estimated by optimization analysis. The estimate of mean sound speed will be verified by comparison to data from CTD measurements.

The remainder of this paper is organized as follows. In Section 2, objective functions for optimization of transponder position estimation with and without knowledge of sound speed are presented. In Section 3, circular and straight-line survey patterns are introduced. In Sections 4 and 5, the constraints for obtaining a unique solution from circular and straight-line surveys are derived, respectively. Section 6 presents and interprets the estimation results of the field experiment. Finally, conclusions are given in Section 7.

2. Position estimation

Recovering the position of a fixed transponder based on acoustic ranges and GPS positions is an inverse problem. Ideally, observations collected at three independent locations can determine the position of a fixed transponder. However, measurement noise deleteriously affects the estimates when only three observations are used for estimation. Therefore, in this study, numerous observations are collected at different locations and then the position of a fixed transponder is estimated by numerical optimization algorithms.

2.1. Estimation when sound speed is observed

Assume the global position of a fixed transponder is $\mathbf{P}_{\mathrm{T}}$:

$$\mathbf{P}_{\mathrm{T}} = [P_{\mathrm{T}x},\ P_{\mathrm{T}y},\ P_{\mathrm{T}z}]^{\mathrm{T}}. \tag{1}$$

The observed slant range and the vessel's GPS position at the ith location are SR_i and $\mathbf{P}_i$, respectively, where

$$\mathbf{P}_i = [P_{ix},\ P_{iy},\ 0]^{\mathrm{T}}. \tag{2}$$

Theoretically, when the sound speed is known and the ray bending effect is ignored, the measured slant range equals the calculated range between points $\mathbf{P}_{\mathrm{T}}$ and $\mathbf{P}_i$:

$$\mathrm{SR}_i = \sqrt{(P_{\mathrm{T}x} - P_{ix})^2 + (P_{\mathrm{T}y} - P_{iy})^2 + (P_{\mathrm{T}z})^2}. \tag{3}$$

However, due to measurement errors, Eq. (3) is not likely to be true. Let the difference between measured and calculated ranges be ε_i:

$$\varepsilon_i = \mathrm{SR}_i - \sqrt{(P_{\mathrm{T}x} - P_{ix})^2 + (P_{\mathrm{T}y} - P_{iy})^2 + (P_{\mathrm{T}z})^2}. \tag{4}$$

By applying an optimization method to this problem, the minimum value of the objective function can be thought of as the summation of square differences ε_i^2. Thus, the objective function is expressed as

$$\text{Minimize} \quad f = \sum_{i=1}^{n} \varepsilon_i^2 = \sum_{i=1}^{n} \left[\text{SR}_i - \sqrt{(P_{\text{T}x} - P_{ix})^2 + (P_{\text{T}y} - P_{iy})^2 + (P_{\text{T}z})^2} \right]^2, \tag{5}$$

where n is the total number of observations.

2.2. Estimation when sound speed is not available

The difficulty in precisely estimating the position of a transponder is the uncertainty of sound speed in the water. Although the sound speed profile can be measured, it is not frequently measured during data collection. Thus, if the mean sound speed V_{a} of the water column is regarded as a variable, the objective function of optimization is rewritten as

$$\text{Minimize} \quad f = \sum_{i=1}^{n} \left[\text{SR}_i - \frac{V_{\text{m}}}{V_{\text{a}}} \sqrt{(P_{\text{T}x} - P_{ix})^2 + (P_{\text{T}y} - P_{iy})^2 + (P_{\text{T}z})^2} \right]^2, \tag{6}$$

where V_{m} is the setting of mean sound speed in an acoustic positioning system for slant range calculation. Usually, V_{m} has a default value of 1500 m/s. The acoustic positioning system utilizes V_{m} and timing information to calculate slant range directly. In total, four variables, $P_{\text{T}x}$, $P_{\text{T}y}$, $P_{\text{T}z}$, and V_{a}, need to be estimated by minimizing the objective function of Eq. (6) from acoustic and GPS observations.

3. Vessel's survey patterns

Acoustic and GPS data are generally collected by moving a vessel in a particular survey pattern. Though a great variety of patterns have been introduced, no common standard exists. However, the survey course must be planned carefully so as to avoid an incorrect or poor estimate of the transponder position. Frequently, circular and straight-line paths are utilized to collect acoustic and GPS observations. These two patterns are presented in Fig. 1, in which $O_{\text{G}}X_{\text{G}}Y_{\text{G}}Z_{\text{G}}$ is the earth-fixed coordinate system with the Y_{G} axis pointing north and the X_{G} axis pointing east.

3.1. Circular survey pattern

For a circular survey pattern, the vessel moves along a circle around the transponder (Fig. 1(a)). The radius of the circular path is r and the position vector of the circle center in the earth-fixed coordinate system is $\mathbf{P}_{\text{c}}$:

$$\mathbf{P}_{\text{c}} = \left[P_{\text{c}x}, \ P_{\text{c}y}, \ 0 \right]^{\text{T}}. \tag{7}$$

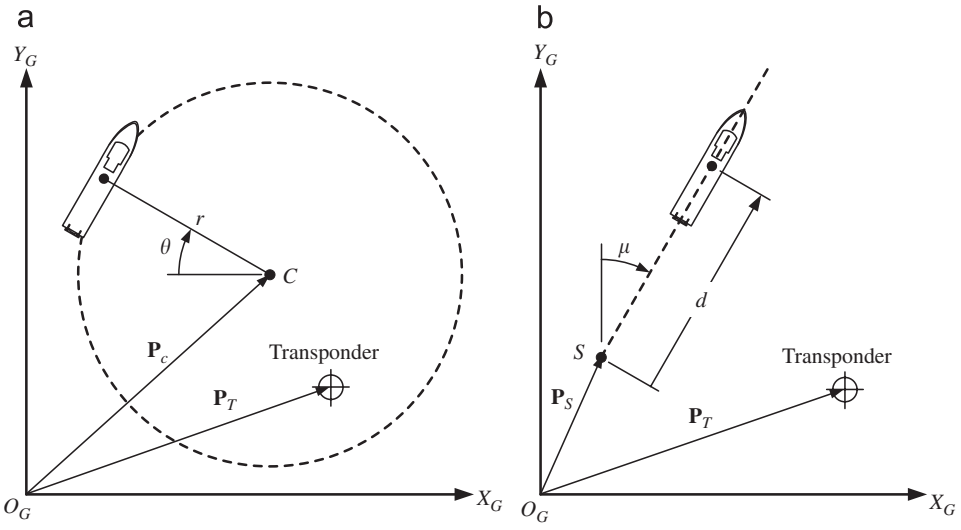

Fig. 1. Coordinate system and schematic for circular and straight-line survey patterns. (a) Circular path and (b) Straight-line path.

In Fig. 1(a), θ is a parameter describing the position of the vessel. Based on the coordinate system in Fig. 1(a), the vessel's GPS position at the ith observation point with corresponding θ_i can be expressed as

$$\mathbf{P}_i^{\mathrm{C}} = \left[P_{ix}^{\mathrm{C}},\ P_{iy}^{\mathrm{C}},\ 0\right]^{\mathrm{T}} = \left[P_{\mathrm{c}x} - r\cos\theta_i,\ P_{\mathrm{c}y} + r\sin\theta_i,\ 0\right]^{\mathrm{T}}, \tag{8}$$

where superscript C indicates the circular survey pattern. The slant range between the seafloor transponder and the observation point can be obtained from Eqs. (1) and (8):

$$\mathrm{SR}_i^{\mathrm{C}} = \sqrt{(P_{\mathrm{T}x} - P_{\mathrm{c}x} + r\cos\theta_i)^2 + (P_{\mathrm{T}y} - P_{\mathrm{c}y} - r\sin\theta_i)^2 + P_{\mathrm{T}z}^2} = t_i V_{\mathrm{a}}, \tag{9}$$

where t_i is the one-way acoustic travel time. However, the measured slant range using the acoustic positioning system is obtained by multiplying the one-way acoustic travel time t_i and sound speed V_{m}. Thus, according to the true slant range expressed in Eq. (9), the slant range measured from the acoustic positioning system is

$$\mathrm{SR}_i^{\mathrm{C}} = t_i V_{\mathrm{m}} = \frac{V_{\mathrm{m}}}{V_{\mathrm{a}}}\sqrt{(P_{\mathrm{T}x} - P_{\mathrm{c}x} + r\cos\theta_i)^2 + (P_{\mathrm{T}y} - P_{\mathrm{c}y} - r\sin\theta_i)^2 + P_{\mathrm{T}z}^2}. \tag{10}$$

3.2. Straight-line survey pattern

For a straight-line survey pattern (Fig. 1(b)), the path starts at location S and continues along a straight line with orientation μ. The position vector of the start point S in the earth-fixed coordinate system is $\mathbf{P}_{\mathrm{s}}$:

$$\mathbf{P}_{\mathrm{s}} = [P_{\mathrm{s}x},\ P_{\mathrm{s}y},\ 0]^{\mathrm{T}}. \tag{11}$$

In Fig. 1(b), d is a parameter describing the position of the vessel. Based on the coordinate system in Fig. 1(b), the vessel's GPS position at the ith observation point with corresponding d_i is represented by

$$\mathbf{P}_i^{\mathrm{L}} = [P_{ix}^{\mathrm{L}},\ P_{iy}^{\mathrm{L}},\ 0]^{\mathrm{T}} = [P_{\mathrm{s}x} + d_i\sin\mu,\ P_{\mathrm{s}y} + d_i\cos\mu,\ 0]^{\mathrm{T}}, \tag{12}$$

where superscript L indicates the straight-line survey pattern. In a straight-line survey, the slant range changes with d. At the ith observation point with corresponding d_i, the slant range between the seafloor transponder and the observation point can be obtained from Eqs. (1) and (12):

$$\mathrm{SR}_i^{\mathrm{L}} = \sqrt{(P_{\mathrm{T}x} - P_{\mathrm{s}x} - d_i\sin\mu)^2 + (P_{\mathrm{T}y} - P_{\mathrm{s}y} - d_i\cos\mu)^2 + P_{\mathrm{T}z}^2} = t_i V_{\mathrm{a}}. \tag{13}$$

Accordingly, the slant range measured by the acoustic positioning system is

$$\mathrm{SR}_i^{\mathrm{L}} = t_i V_{\mathrm{m}} = \frac{V_{\mathrm{m}}}{V_{\mathrm{a}}}\sqrt{(P_{\mathrm{T}x} - P_{\mathrm{s}x} - d_i\sin\mu)^2 + (P_{\mathrm{T}y} - P_{\mathrm{s}y} - d_i\cos\mu)^2 + P_{\mathrm{T}z}^2}. \tag{14}$$

4. Constraints on circular survey pattern

An inappropriate survey path results in either convergence failures in numerical iteration or non-unique solutions for the inverse problem of transponder localization. This section examines the constraints that provide unique solutions to transponder localization for the circular survey pattern. Studies are performed under the assumptions that the vessel is precisely steered along a circular path and observations are collected without any measurement or system error. Additionally, due to the relatively short range of sound propagation between the seafloor transponder and surface observation point, sound ray bending in shallow water is negligible.

4.1. Survey when sound speed is observed

Suppose the survey is conducted along a circle with radius r and precise vertical sound speed profiles of the water column are observed during the survey. Based on the objective function in Eq. (5) and the true slant range in Eq. (9), parameters SR_i, $P_{\mathrm{c}x}$, $P_{\mathrm{c}y}$, r, and θ_i are given, and parameters $P_{\mathrm{T}x}$, $P_{\mathrm{T}y}$, and $P_{\mathrm{T}z}$ are the optimization variables. Prior to optimization, the existence and uniqueness of solutions must be checked. Based on Eq. (9), the functions related to the true slant ranges collected at different observation points θ_i are expressed as

$$f_i = SR_i^2 - [(P_{\mathrm{T}x} - P_{\mathrm{c}x} + r\cos\theta_i)^2 + (P_{\mathrm{T}y} - P_{\mathrm{c}y} - r\sin\theta_i)^2 + P_{\mathrm{T}z}^2] = 0, \quad i = 1, 2, \ldots, n. \tag{15}$$

In this system of equations, there are three unknown variables. The solution of the problem is guaranteed to exist when the Jacobian $\partial(f_1, f_2, \ldots, f_n)/\partial(P_{\mathrm{T}x}, P_{\mathrm{T}y}, P_{\mathrm{T}z})$ of these functions is of rank 3. This fact follows from the implicit function theorem (Hildebrand, 1976). Furthermore, at least three functions of f_i must be independent to provide a unique solution. Based on

Eq. (15), the Jacobian matrix of any three functions, say, f_1, f_2, and f_3, with respect to variables P_{Tx}, P_{Ty}, and P_{Tz} is given by

$$\mathbf{J}_f(P_{Tx},P_{Ty},P_{Tz})=\frac{\partial(f_1,f_2,f_3)}{\partial(P_{Tx},P_{Ty},P_{Tz})} = -8P_{Tz}\begin{bmatrix} P_{Tx}-P_{cx}+r\cos\theta_1 & P_{Ty}-P_{cy}-r\sin\theta_1 & 1\\ P_{Tx}-P_{cx}+r\cos\theta_2 & P_{Ty}-P_{cy}-r\sin\theta_2 & 1\\ P_{Tx}-P_{cx}+r\cos\theta_3 & P_{Ty}-P_{cy}-r\sin\theta_3 & 1\end{bmatrix}. \tag{16}$$

The Jacobian matrix of Eq. (16) is of rank 3, and the Jacobian determinant yields

$$|\mathbf{J}_f(e_x,e_y,P_{Tz})| = -8r^2P_{Tz}[\sin(\theta_1-\theta_2)+\sin(\theta_2-\theta_3)+\sin(\theta_3-\theta_1)]. \tag{17}$$

Apparently, the Jacobian determinant does not vanish when θ_1, θ_2, and θ_3 are different. Consequently, acoustic and GPS observations collected along a single circle can determine parameters P_{Tx}, P_{Ty}, and P_{Tz} uniquely.

4.2. Survey when sound speed is not available

When sound speed along a vertical acoustic path is unknown, the mean sound speed V_a is treated as an unknown parameter in the optimization problem. According to the objective function in Eq. (6) and the measured slant range obtained by Eq. (10), parameters SR_i, P_{cx}, P_{cy}, r, θ_i, and V_m are known, and parameters P_{Tx}, P_{Ty}, P_{Tz}, and V_a are the optimization variables.

Suppose observations are collected along a circle with radius r. According to Eq. (10), the functions associated with the measured slant ranges at different observation points θ_i can be expressed as

$$f_i = SR_i^2-\left(\frac{V_m}{V_a}\right)^2[(P_{Tx}-P_{cx}+r\cos\theta_i)^2+(P_{Ty}-P_{cy}-r\sin\theta_i)^2+P_{Tz}^2]=0 \quad i=1,2,\ldots,n. \tag{18}$$

In this system of equations, there are four unknown variables. The system has a unique solution if the Jacobian of these functions is of rank 4, and at least four functions of f_i are independent. Based on Eq. (18), the Jacobian matrix of any four functions, say, f_1, f_2, f_3, and f_4, with respect to variables P_{Tx}, P_{Ty}, P_{Tz} and V_a is given by

$$\begin{aligned}\mathbf{J}_f(P_{Tx},P_{Ty},P_{Tz},V_a)&=\frac{\partial(f_1,f_2,f_3,f_4)}{\partial(P_{Tx},P_{Ty},P_{Tz},V_a)}\\ &=-16P_{Tz}\frac{V_m^8}{V_a^9}\begin{bmatrix} P_{Tx}-P_{cx}+r\cos\theta_1 & P_{Ty}-P_{cy}-r\sin\theta_1 & 1 & (P_{Tx}-P_{cx}+r\cos\theta_1)^2+(P_{Ty}-P_{cy}-r\sin\theta_1)^2+P_{Tz}^2\\ P_{Tx}-P_{cx}+r\cos\theta_2 & P_{Ty}-P_{cy}-r\sin\theta_2 & 1 & (P_{Tx}-P_{cx}+r\cos\theta_2)^2+(P_{Ty}-P_{cy}-r\sin\theta_2)^2+P_{Tz}^2\\ P_{Tx}-P_{cx}+r\cos\theta_3 & P_{Ty}-P_{cy}-r\sin\theta_3 & 1 & (P_{Tx}-P_{cx}+r\cos\theta_3)^2+(P_{Ty}-P_{cy}-r\sin\theta_3)^2+P_{Tz}^2\\ P_{Tx}-P_{cx}+r\cos\theta_4 & P_{Ty}-P_{cy}-r\sin\theta_4 & 1 & (P_{Tx}-P_{cx}+r\cos\theta_4)^2+(P_{Ty}-P_{cy}-r\sin\theta_4)^2+P_{Tz}^2\end{bmatrix}.\end{aligned} \tag{19}$$

From Eq. (19), the Jacobian matrix is of rank 3 and the Jacobian determinant everywhere is zero. This result implies that P_{Tx}, P_{Ty}, P_{Tz} and V_a cannot be determined uniquely from observations collected along a circle. Fortunately, the dependence among observations can be eliminated when the survey is conducted along two circles with different radii. Suppose the survey is conducted along two circles with radii r_1 and r_2. Four observations are collected, in which, for example, one is collected along a circle with radius r_1 at point θ_1 and the other three are collected along a circle with radius r_2 at points θ_2, θ_3, and θ_4. The system of equations can then be established:

$$\begin{aligned} f_1 &= SR_1^2-\left(\frac{V_m}{V_a}\right)^2[(P_{Tx}-P_{cx}+r_1\cos\theta_1)^2+(P_{Ty}-P_{cy}-r_1\sin\theta_1)^2+P_{Tz}^2],\\ f_2 &= SR_2^2-\left(\frac{V_m}{V_a}\right)^2[(P_{Tx}-P_{cx}+r_2\cos\theta_2)^2+(P_{Ty}-P_{cy}-r_2\sin\theta_2)^2+P_{Tz}^2],\\ f_3 &= SR_3^2-\left(\frac{V_m}{V_a}\right)^2[(P_{Ty}-P_{cy}-r_2\cos\theta_3)^2+(P_{Ty}-P_{cy}-r_2\sin\theta_3)^2+P_{Tz}^2],\\ f_4 &= SR_4^2-\left(\frac{V_m}{V_a}\right)^2[(P_{Tx}-P_{cx}+r_2\cos\theta_4)^2+(P_{Ty}-P_{cy}-r_2\sin\theta_4)^2+P_{Tz}^2]. \end{aligned} \tag{20}$$

According to Eq. (20), the Jacobian matrix is written as

$$\mathbf{J}_f(P_{\mathrm{T}x}, P_{\mathrm{T}y}, P_{\mathrm{T}z}, V_{\mathrm{a}}) = -16P_{\mathrm{T}z}\frac{V_{\mathrm{m}}^8}{V_{\mathrm{a}}^9}\begin{bmatrix} P_{\mathrm{T}x}-P_{\mathrm{c}x}+r_1\cos\theta_1 & P_{\mathrm{T}y}-P_{\mathrm{c}y}-r_1\sin\theta_1 & 1 & (P_{\mathrm{T}x}-P_{\mathrm{c}x}+r_1\cos\theta_1)^2+(P_{\mathrm{T}y}-P_{\mathrm{c}y}-r_1\sin\theta_1)^2+P_{\mathrm{T}z}^2 \\ P_{\mathrm{T}x}-P_{\mathrm{c}x}+r_2\cos\theta_2 & P_{\mathrm{T}y}-P_{\mathrm{c}y}-r_2\sin\theta_2 & 1 & (P_{\mathrm{T}x}-P_{\mathrm{c}x}+r_2\cos\theta_2)^2+(P_{\mathrm{T}y}-P_{\mathrm{c}y}-r_2\sin\theta_2)^2+P_{\mathrm{T}z}^2 \\ P_{\mathrm{T}x}-P_{\mathrm{c}x}+r_2\cos\theta_3 & P_{\mathrm{T}y}-P_{\mathrm{c}y}-r_2\sin\theta_3 & 1 & (P_{\mathrm{T}x}-P_{\mathrm{c}x}+r_2\cos\theta_3)^2+(P_{\mathrm{T}y}-P_{\mathrm{c}y}-r_2\sin\theta_3)^2+P_{\mathrm{T}z}^2 \\ P_{\mathrm{T}x}-P_{\mathrm{c}x}+r_2\cos\theta_4 & P_{\mathrm{T}y}-P_{\mathrm{c}y}-r_2\sin\theta_4 & 1 & (P_{\mathrm{T}x}-P_{\mathrm{c}x}+r_2\cos\theta_4)^2+(P_{\mathrm{T}y}-P_{\mathrm{c}y}-r_2\sin\theta_4)^2+P_{\mathrm{T}z}^2 \end{bmatrix}. \tag{21}$$

The Jacobian matrix in Eq. (21) is of rank 4, and the Jacobian determinant generates

$$|\mathbf{J}_f(P_{\mathrm{T}x}, P_{\mathrm{T}y}, P_{\mathrm{T}z}, V_{\mathrm{a}})| = 16r_2^2(r_1^2-r_2^2)P_{\mathrm{T}z}\frac{V_{\mathrm{m}}^8}{V_{\mathrm{a}}^9}[\sin(\theta_2-\theta_3)+\sin(\theta_3-\theta_4)+\sin(\theta_4-\theta_2)]. \tag{22}$$

If $r_1 \neq r_2$ and θ_2, θ_3, and θ_4 are different, the Jacobian determinant of Eq. (22) will not vanish. Consequently, parameters $P_{\mathrm{T}x}$, $P_{\mathrm{T}y}$, $P_{\mathrm{T}z}$ and V_{a} can be determined uniquely when the survey is conducted along two circles with different radii.

5. Constraints on straight-line survey

This section presents a discussion of constraints to provide unique solutions to transponder localization for the straight-line survey pattern. Studies are conducted under the assumptions that the vessel is steered along a straight-line path precisely, and observations are collected with no measurement or system error. Furthermore, sound ray bending in shallow water is assumed to be negligible.

5.1. Survey when sound speed is observed

Suppose the vertical sound speed profiles of the water column are known during the survey. According to the objective function in Eq. (5) and true slant range in Eq. (13), parameters SR_i, μ, $P_{\mathrm{s}x}$, $P_{\mathrm{s}y}$, and d_i are known, and parameters $P_{\mathrm{T}x}$, $P_{\mathrm{T}y}$, and $P_{\mathrm{T}z}$ are optimization variables. According to Eq. (13), the functions related to true slant ranges at different observation points d_i are

$$f_i = \mathrm{SR}_i^2 - [(P_{\mathrm{T}x}-P_{\mathrm{s}x}-d_i\sin\mu)^2+(P_{\mathrm{T}y}-P_{\mathrm{s}y}-d_i\cos\mu)^2+P_{\mathrm{T}z}^2] = 0, \quad i = 1,2,\ldots,n. \tag{23}$$

The Jacobian matrix of any three functions, say, f_1, f_2, and f_3, with respect to variables $P_{\mathrm{T}x}$, $P_{\mathrm{T}y}$, and $P_{\mathrm{T}z}$ is given by

$$J_f(P_{\mathrm{T}x}, P_{\mathrm{T}y}, P_{\mathrm{T}z}) = -8P_{\mathrm{T}z}\begin{bmatrix} P_{\mathrm{T}x}-P_{\mathrm{s}x}-d_1\sin\mu & P_{\mathrm{T}y}-P_{\mathrm{s}y}-d_1\cos\mu & 1 \\ P_{\mathrm{T}x}-P_{\mathrm{s}x}-d_2\sin\mu & P_{\mathrm{T}y}-P_{\mathrm{s}y}-d_2\cos\mu & 1 \\ P_{\mathrm{T}x}-P_{\mathrm{s}x}-d_3\sin\mu & P_{\mathrm{T}y}-P_{\mathrm{s}y}-d_3\cos\mu & 1 \end{bmatrix}. \tag{24}$$

The Jacobian matrix in Eq. (24) is of rank 2 and the Jacobian determinant yields

$$|\mathbf{J}_f(P_{\mathrm{T}x}, P_{\mathrm{T}y}, P_{\mathrm{T}z})| = 0. \tag{25}$$

These analytical results demonstrate that there are an infinite number of solutions for $P_{\mathrm{T}x}$, $P_{\mathrm{T}y}$, and $P_{\mathrm{T}z}$. That is, the transponder cannot be uniquely located from observations collected along a straight line.

Fortunately, the dependence among observations can be resolved by conducting a survey along two different straight-line paths. Suppose one observation is collected at location d_1 on a straight-line path with orientation angle μ_1 through ($P_{\mathrm{s}x1}$, $P_{\mathrm{s}y1}$), and the other two observations are collected at locations d_2 and d_3 on another straight-line path with orientation angle μ_2 through ($P_{\mathrm{s}x2}$, $P_{\mathrm{s}y2}$). The system of equations for the three parameters of $P_{\mathrm{T}x}$, $P_{\mathrm{T}y}$, and $P_{\mathrm{T}z}$ can then be established:

$$\begin{aligned} f_1 &= SR_1^2 - [(P_{\mathrm{T}x}-P_{\mathrm{s}x1}-d_1\sin\mu_1)^2+(P_{\mathrm{T}y}-P_{\mathrm{s}y1}-d_1\cos\mu_1)^2+P_{\mathrm{T}z}^2], \\ f_2 &= SR_2^2 - [(P_{\mathrm{T}x}-P_{\mathrm{s}x2}-d_2\sin\mu_2)^2+(P_{\mathrm{T}y}-P_{\mathrm{s}y2}-d_2\cos\mu_2)^2+P_{\mathrm{T}z}^2], \\ f_3 &= SR_3^2 - [(P_{\mathrm{T}x}-P_{\mathrm{s}x2}-d_3\sin\mu_2)^2+(P_{\mathrm{T}y}-P_{\mathrm{s}y2}-d_3\cos\mu_2)^2+P_{\mathrm{T}z}^2]. \end{aligned} \tag{26}$$

Accordingly, the Jacobian matrix is written as

$$\mathbf{J}_f(P_{\mathrm{T}x}, P_{\mathrm{T}y}, P_{\mathrm{T}z}) = -8P_{\mathrm{T}z}\begin{bmatrix} P_{\mathrm{T}x} - P_{\mathrm{s}x1} - d_1 \sin\mu_1 & P_{\mathrm{T}y} - P_{\mathrm{s}y1} - d_1 \cos\mu_1 & 1 \\ P_{\mathrm{T}x} - P_{\mathrm{s}x2} - d_2 \sin\mu_2 & P_{\mathrm{T}y} - P_{\mathrm{s}y2} - d_2 \cos\mu_2 & 1 \\ P_{\mathrm{T}x} - P_{\mathrm{s}x2} - d_3 \sin\mu_2 & P_{\mathrm{T}y} - P_{\mathrm{s}y2} - d_3 \cos\mu_2 & 1 \end{bmatrix}. \tag{27}$$

The Jacobian matrix in Eq. (27) is of rank 3, and the Jacobian determinant yields

$$|\mathbf{J}_f(P_{\mathrm{T}x}, P_{\mathrm{T}y}, P_{\mathrm{T}z})| = (d_3 - d_2)[(P_{sx2} - P_{sx1})\cos\mu_2 - (P_{sy2} - P_{sy1})\sin\mu_2 + d_1\sin(\mu_2 - \mu_1)]. \tag{28}$$

The Jacobian determinant in Eq. (28) will not vanish when three observation points are not collinear. Consequently, parameters $P_{\mathrm{T}x}$, $P_{\mathrm{T}y}$, and $P_{\mathrm{T}z}$ can be determined uniquely when the survey is conducted along two different straight-line paths.

5.2. Survey when sound speed is not available

In the case where sound speed along a vertical acoustic path is not known, the mean sound speed V_{a} is treated as an unknown parameter in the optimization problem. That is, parameters $P_{\mathrm{T}x}$, $P_{\mathrm{T}y}$, $P_{\mathrm{T}z}$, and V_{a} are optimization variables. Based on Eq. (14), the functions related to measured slant ranges at different observation points d_i are

$$f_i = SR_i^2 - \left(\frac{V_{\mathrm{m}}}{V_{\mathrm{a}}}\right)^2[(P_{\mathrm{T}x} - P_{\mathrm{s}x} - d_i\sin\mu)^2 + (P_{\mathrm{T}y} - P_{\mathrm{s}y} - d_i\cos\mu)^2 + P_{\mathrm{T}z}^2] = 0, \quad i = 1, 2, \ldots, n. \tag{29}$$

The Jacobian matrix of any four functions, say, f_1, f_2, f_3 and f_4, with respect to variables $P_{\mathrm{T}x}$, $P_{\mathrm{T}y}$, $P_{\mathrm{T}z}$ and V_{a} is given by

$$\begin{aligned}\mathbf{J}_f(P_{\mathrm{T}x}, P_{\mathrm{T}y}, P_{\mathrm{T}z}, V_{\mathrm{a}}) &= \frac{\partial(f_1, f_2, f_3, f_4)}{\partial(P_{\mathrm{T}x}, P_{\mathrm{T}y}, P_{\mathrm{T}z}, V_{\mathrm{a}})} \\ &= -16P_{\mathrm{T}z}\frac{V_{\mathrm{m}}^8}{V_{\mathrm{a}}^9}\begin{bmatrix} P_{\mathrm{T}x} - P_{\mathrm{s}x} - d_1\sin\mu & P_{\mathrm{T}y} - P_{\mathrm{s}y} - d_1\cos\mu & 1 & (P_{\mathrm{T}x} - P_{\mathrm{s}x} - d_1\sin\mu)^2 + (P_{\mathrm{T}y} - P_{\mathrm{s}y} - d_1\cos\mu)^2 + P_{\mathrm{T}z}^2 \\ P_{\mathrm{T}x} - P_{\mathrm{s}x} - d_2\sin\mu & P_{\mathrm{T}y} - P_{\mathrm{s}y} - d_2\cos\mu & 1 & (P_{\mathrm{T}x} - P_{\mathrm{s}x} - d_2\sin\mu)^2 + (P_{\mathrm{T}y} - P_{\mathrm{s}y} - d_2\cos\mu)^2 + P_{\mathrm{T}z}^2 \\ P_{\mathrm{T}x} - P_{\mathrm{s}x} - d_3\sin\mu & P_{\mathrm{T}y} - P_{\mathrm{s}y} - d_3\cos\mu & 1 & (P_{\mathrm{T}x} - P_{\mathrm{s}x} - d_3\sin\mu)^2 + (P_{\mathrm{T}y} - P_{\mathrm{s}y} - d_3\cos\mu)^2 + P_{\mathrm{T}z}^2 \\ P_{\mathrm{T}x} - P_{\mathrm{s}x} - d_4\sin\mu & P_{\mathrm{T}y} - P_{\mathrm{s}y} - d_4\cos\mu & 1 & (P_{\mathrm{T}x} - P_{\mathrm{s}x} - d_4\sin\mu)^2 + (P_{\mathrm{T}y} - P_{\mathrm{s}y} - d_4\cos\mu)^2 + P_{\mathrm{T}z}^2 \end{bmatrix}.\end{aligned} \tag{30}$$

From Eq. (30), it follows that the Jacobian determinant everywhere is zero and the Jacobian matrix is of rank 3. This result implies that $P_{\mathrm{T}x}$, $P_{\mathrm{T}y}$, $P_{\mathrm{T}z}$, and V_{a} cannot be uniquely determined from observations collected along a straight line.

As proposed in Section 5.1, observations collected along two different straight-line paths can exactly locate the transponder position (P_{Tx}, $P_{\mathrm{T}y}$, and $P_{\mathrm{T}z}$). Observations collected along two different straight-line paths may also uniquely determine the transponder position and V_{a}. To investigate this possibility, we assume that three observations are collected at points d_1, d_2, and d_3 on a straight-line path with orientation angle μ_2 through ($P_{\mathrm{s}x2}$, $P_{\mathrm{s}y2}$), and one observation is collected at point d_4 on another straight-line path with orientation angle μ_1 through ($P_{\mathrm{s}x1}$, $P_{\mathrm{s}y1}$). The system of equations for the four parameters $P_{\mathrm{T}x}$, $P_{\mathrm{T}y}$, $P_{\mathrm{T}z}$ and V_{a} are then established:

$$\begin{aligned} f_1 &= SR_1^2 - \left(\frac{V_{\mathrm{m}}}{V_{\mathrm{a}}}\right)^2[(P_{\mathrm{T}x} - P_{\mathrm{s}x1} - d_1\sin\mu_1)^2 + (P_{\mathrm{T}y} - P_{\mathrm{s}y1} - d_1\cos\mu_1)^2 + P_{\mathrm{T}z}^2], \\ f_2 &= SR_2^2 - \left(\frac{V_{\mathrm{m}}}{V_{\mathrm{a}}}\right)^2[(P_{\mathrm{T}x} - P_{\mathrm{s}x1} - d_2\sin\mu_1)^2 + (P_{\mathrm{T}y} - P_{\mathrm{s}y1} - d_2\cos\mu_1)^2 + P_{\mathrm{T}z}^2], \\ f_3 &= SR_3^2 - \left(\frac{V_{\mathrm{m}}}{V_{\mathrm{a}}}\right)^2[(P_{\mathrm{T}x} - P_{\mathrm{s}x1} - d_3\sin\mu_1)^2 + (P_{\mathrm{T}y} - P_{\mathrm{s}y1} - d_3\cos\mu_1)^2 + P_{\mathrm{T}z}^2], \\ f_4 &= SR_4^2 - \left(\frac{V_{\mathrm{m}}}{V_{\mathrm{a}}}\right)^2[(P_{\mathrm{T}x} - P_{\mathrm{s}x2} - d_4\sin\mu_2)^2 + (P_{\mathrm{T}y} - P_{\mathrm{s}y2} - d_4\cos\mu_2)^2 + P_{\mathrm{T}z}^2]. \end{aligned} \tag{31}$$

Accordingly, the Jacobian matrix is written as

$$J_f(P_{Tx}, P_{Ty}, P_{Tz}, V_a) = \frac{\partial(f_1, f_2, f_3, f_4)}{\partial(P_{Tx}, P_{Ty}, P_{Tz}, V_a)}$$
$$= -16P_{Tz}\frac{V_m^8}{V_a^9}\begin{bmatrix} P_{Tx}-P_{sx1}-d_1\sin\mu_1 & P_{Ty}-P_{sy1}-d_1\cos\mu_1 & 1 & (P_{Tx}-P_{sx1}-d_1\sin\mu_1)^2+(P_{Ty}-P_{sy1}-d_1\cos\mu_1)^2+P_{Tz}^2 \\ P_{Tx}-P_{sx1}-d_2\sin\mu_1 & P_{Ty}-P_{sy1}-d_2\cos\mu_1 & 1 & (P_{Tx}-P_{sx1}-d_2\sin\mu_1)^2+(P_{Ty}-P_{sy1}-d_2\cos\mu_1)^2+P_{Tz}^2 \\ P_{Tx}-P_{sx1}-d_3\sin\mu_1 & P_{Ty}-P_{sy1}-d_3\cos\mu_1 & 1 & (P_{Tx}-P_{sx1}-d_3\sin\mu_1)^2+(P_{Ty}-P_{sy1}-d_3\cos\mu_1)^2+P_{Tz}^2 \\ P_{Tx}-P_{sx2}-d_4\sin\mu_2 & P_{Ty}-P_{sy2}-d_4\cos\mu_2 & 1 & (P_{Tx}-P_{sx2}-d_4\sin\mu_2)^2+(P_{Ty}-P_{sy2}-d_4\cos\mu_2)^2+P_{Tz}^2 \end{bmatrix}. \quad (32)$$

The Jacobian matrix in Eq. (32) is of rank 4, and the Jacobian determinant yields

$$|\mathbf{J}_f(P_{Tx}, P_{Ty}, P_{Tz}, V_a)| = (d_1-d_2)(d_2-d_3)(d_3-d_1)[(P_{sx2}-P_{sx1})\cos\mu_1 - (P_{sy2}-P_{sy1})\sin\mu_1 + d_4\sin(\mu_2-\mu_1)]. \quad (33)$$

Obviously, the Jacobian determinant will not vanish when the survey is conducted along two straight-line paths.

6. Field experiment at sea

On August 21, 2006, a field experiment was conducted at approximately 22°32′N, 120°6′E, roughly 20 km west of Kaohsiung Harbor, Taiwan. The mooring of the transponder (Fig. 2(a)) was deployed at a water depth of about 350 m using Ocean Researcher III, a research vessel operated by the National Sun Yat-sen University. The sensors used for collecting data were a commercial USBL positioning system not designed for precise ranging, a commercial GPS, a Gyro compass, and a motion sensor. Table 1 lists the specific features of these instruments. The onboard USBL transceiver was mounted at the end of a pole located over the ship's side (Fig. 2(b)). The position of the onboard acoustic transceiver was calculated based on the GPS position and attitude (yaw, roll, and pitch) of the research vessel.

Seawater properties including salinity, temperature, and density were measured at the experimental area before and after the surveys. Fig. 3 presents these two CTD measurement results and CTD-derived sound speed profiles. The local sound speed profile is calculated using the Chen–Millero equation (Chen and Millero, 1977). The harmonic mean sound speed before and after the surveys are 1520.68 and 1521.31 m/s, respectively. Straight-line survey was conducted first near the top of the moored transponder. Then circular survey followed. Fig. 4 shows the vessel tracks, which are simply segmented into eight straight-line paths and four circular paths. The eight straight-line paths are labeled L1–8, and the four circular paths are labeled C1–4. In total, the straight-line survey and circular survey collected 1515 and 1349 acoustic and GPS observations, respectively, over a period of 110 min.

6.1. Position estimates

The vessel's GPS observations were recorded and then computed in the WGS84 reference frame. The location of the seafloor transponder was first estimated with a constant sound speed (V_a) of 1521 m/s, which was the mean value resulting from two CTD measurements. According to Eq. (5), optimization evaluations were carried out for observations collected from any two segmented paths. Tables 2 and 3 show the optimal results, in which standard deviations of estimates P_{Tx}, P_{Ty}, and P_{Tz} are less than 1 m. However, the difference in the estimates of P_{Tx} between those obtained from the straight-line survey and those from the circular survey is about 3 m. In addition, from Tables 2 and 3, we can see the estimates of P_{Tx} decrease gradually over the survey period. It is well known that the performance of GPS varies systematically with time and satellite geometry. The dominant direction of orbital motion of GPS satellites from north to south causes the east–west coordinates to have a lower accuracy than north–south coordinates (Bevis et al., 1995; Saab and Charbachy, 2000). Therefore, the long-term errors in P_{Tx} may be due to the known weakness in resolving GPS east–west coordinates. One possible remedy for this problem is to increase survey duration (Shiobara et al., 1997; Spiess et al., 1998).

By regarding the mean sound speed as an unknown, the optimum evaluations based on Eq. (6) were performed for observations collected from any two segmented paths. Tables 4 and 5 present the optimal estimates of the transponder position and mean sound speed. The optimal estimates of the transponder position are consistent with those obtained from observations with known sound speed. Additionally, the estimates of the mean sound speeds resulting from the straight-line and circular surveys are in agreement with the CTD-derived mean sound speed of 1521 m/s. Standard deviations of estimates for P_{Tx}, P_{Ty}, and P_{Tz} are less than 1 m; however, due to the GPS drift error—as discussed earlier—the variation in the estimates of P_{Tx} is considerably greater than that in the estimates of P_{Ty}.

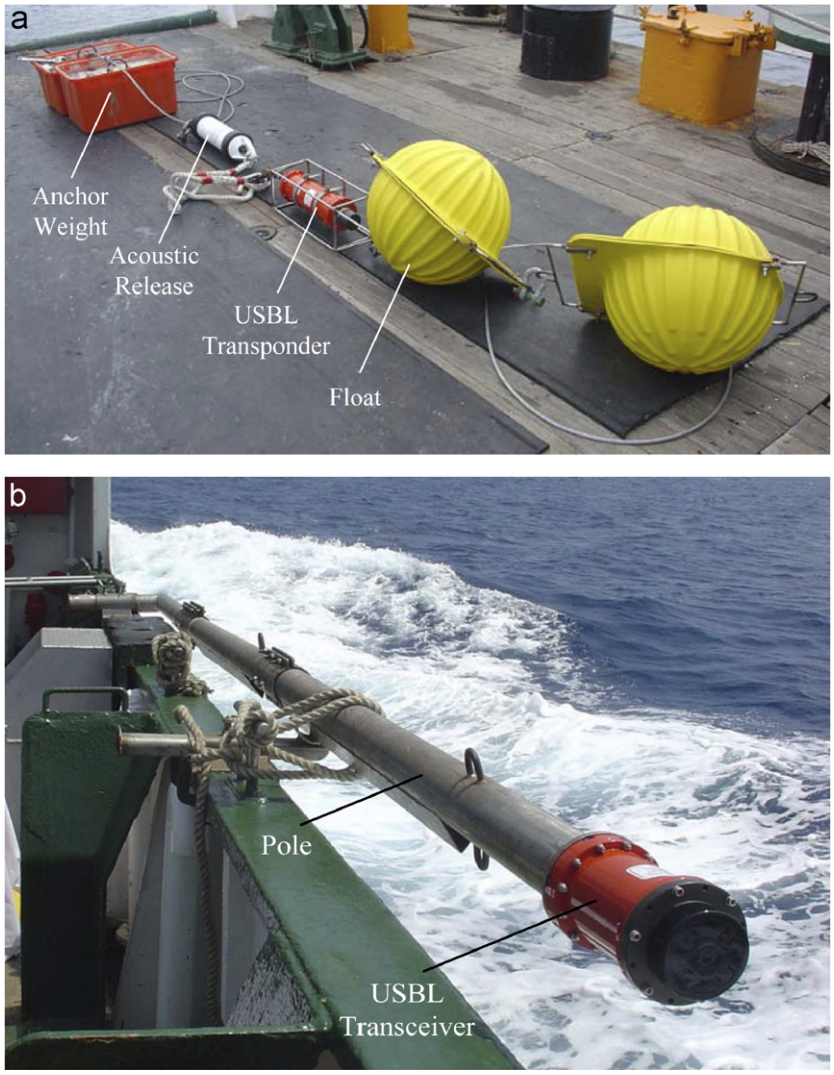

Fig. 2. The acoustic ranging system. (a) The mooring of the transponder was deployed approximately 20 km off shoreline at Kaohsiung Harbor for measuring the slant range from the transceiver mounted on the vessel. (b) The USBL transceiver was mounted at the end of a 5-m-long pole and fixed on the side of the observation vessel.

Table 1
Description of the instrumentation used to measure acoustic range, GPS position, and vessel attitude

Instrument	Update rate (Hz)	Precision	Range
USBL positioning system	0.67	Slant range: 0.2 m	Slant range: 1000 m Beamwidth: $\pm 60^\circ$
GPS	1	1 m	–
Gyro compass	10	0.05° RMS secant latitude	360°
Motion sensor	30	Pitch: 0.04°	Pitch: $\pm 60^\circ$
		Roll: 0.04°	Roll: $\pm 60^\circ$
		Heave: 5 cm	Heave: ± 10 m

6.2. Number of observations

This study provides a theoretical proof that observations collected from two straight-line paths are required to uniquely estimate transponder position and mean sound speed. In statistical practice, the accuracy of estimates increases with increasing numbers of observations. However, having more observations means lengthening the time period over which

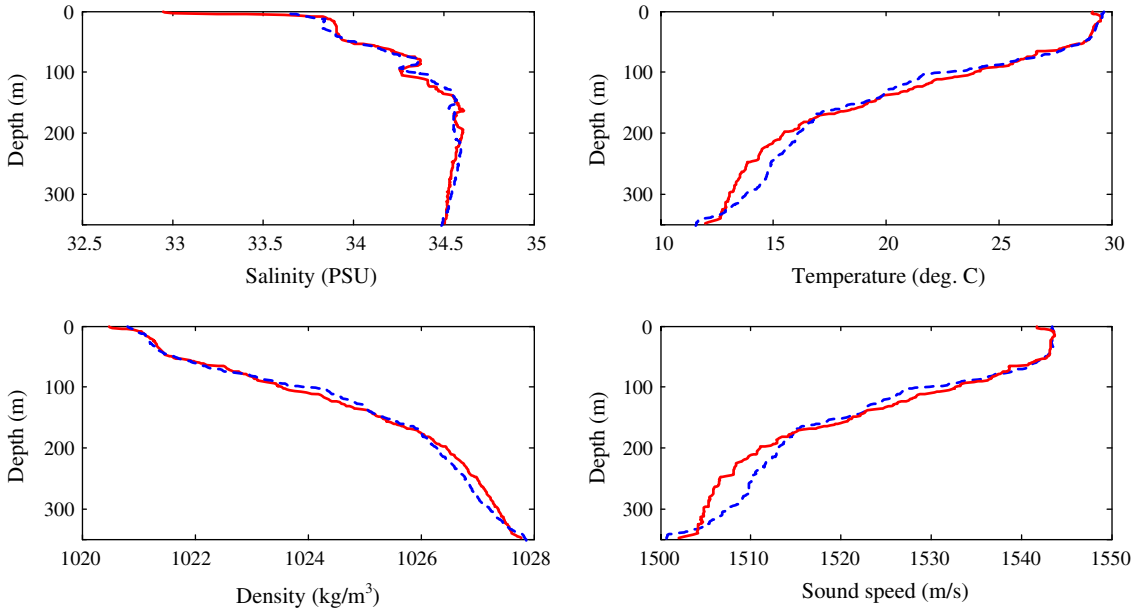

Fig. 3. Vertical profiles of water salinity, temperature, density, and CTD-derived sound speed. The solid lines are profiles measured before the survey, and the dashed lines are profiles measured after the survey.

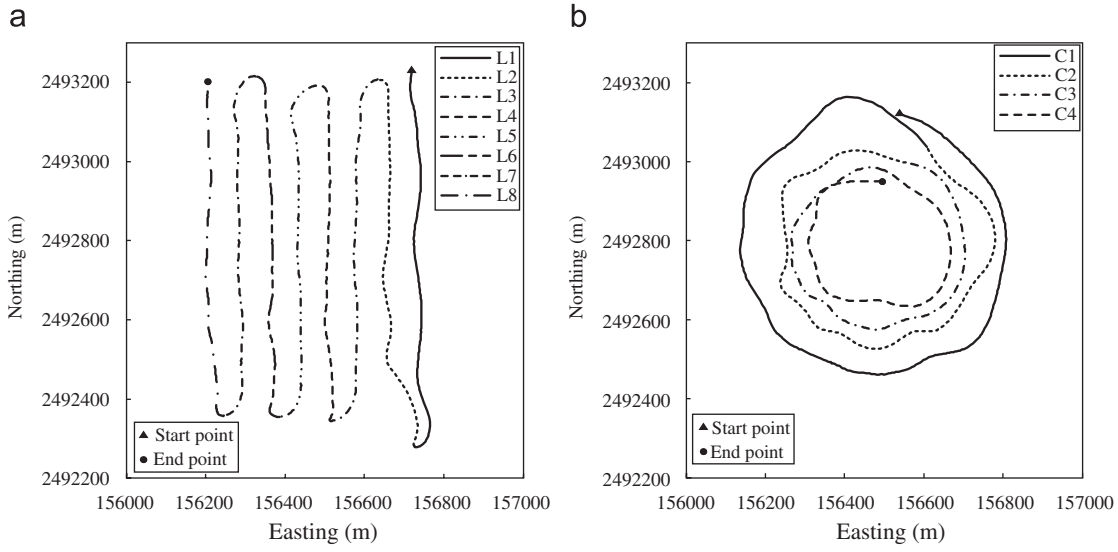

Fig. 4. The plot presents the vessel tracks during the acoustic ranging. The vessel tracks are segmented into (a) eight straight-line paths and (b) four circular paths.

data is collected. Therefore, a positioning system may need to identify the minimum number of observations required to ensure a desired accuracy in transponder position estimation. Table 4 lists the optimal estimates obtained with observations collected from any two segmented paths. In the same manner, optimizations were performed with observations collected from any three, four, five, six, and seven segmented paths. Fig. 5 shows the mean values and standard deviations for the optimal estimates corresponding to different numbers of segmented paths. In Fig. 5, the variations of mean values of transponder position and mean sound speed with the number of segmented paths are within 10 cm and 1 m/s, respectively. Just as expected, the standard deviations of transponder position and mean sound speed decrease as the number of segmented paths increases. To attain a specific positioning accuracy (1σ), the required number of segmented paths can be roughly determined from Fig. 5. For instance, if transponder-positioning accuracy of 0.5 m is desired, the required minimum number of segmented paths is four.

Table 2
Optimal estimates of the transponder position using acoustic and GPS observations collected from two segmented straight-line paths

Straight-line paths	P_{Tx} (m)	P_{Ty} (m)	P_{Tz} (m)
L1, L2	156464.97	2492807.95	−342.92
L1, L3	156465.34	2492807.93	−343.15
L1, L4	156465.33	2492807.91	−343.15
L1, L5	156465.11	2492807.78	−342.99
L1, L6	156464.90	2492807.79	−342.83
L1, L7	156464.88	2492807.79	−342.81
L1, L8	156464.41	2492808.07	−342.40
L2, L3	156464.98	2492807.92	−342.99
L2, L4	156465.14	2492807.89	−343.11
L2, L5	156464.95	2492807.79	−342.99
L2, L6	156464.75	2492807.80	−342.86
L2, L7	156464.75	2492807.79	−342.87
L2, L8	156464.24	2492808.03	−342.52
L3, L4	156465.50	2492807.87	−343.19
L3, L5	156464.94	2492807.77	−343.03
L3, L6	156464.62	2492807.78	−342.92
L3, L7	156464.67	2492807.78	−342.94
L3, L8	156464.03	2492808.07	−342.69
L4, L5	156464.42	2492807.73	−343.06
L4, L6	156464.25	2492807.74	−343.03
L4, L7	156464.44	2492807.74	−343.04
L4, L8	156463.69	2492807.98	−342.93
L5, L6	156463.82	2492807.63	−343.14
L5, L7	156464.40	2492807.61	−343.08
L5, L8	156463.38	2492807.91	−343.16
L6, L7	156464.65	2492807.64	−342.93
L6, L8	156463.13	2492807.90	−343.35
L7, L8	156461.14	2492807.90	−344.80
Mean value	156464.46	2492807.84	−343.03
Standard deviation	0.869	0.122	0.399

The CTD derived mean sound speed is 1521.0 m/s.

Table 3
Optimal estimates of the transponder position using acoustic and GPS observations collected from two segmented circular paths

Circular paths	P_{Tx} (m)	P_{Ty} (m)	P_{Tz} (m)
C1, C2	156462.27	2492807.24	−342.71
C1, C3	156462.29	2492807.29	−342.65
C1, C4	156462.31	2492807.23	−342.76
C2, C3	156461.29	2492806.92	−342.77
C2, C4	156461.22	2492806.85	−342.83
C3, C4	156460.75	2492806.70	−342.85
Mean value	156461.69	2492807.04	−342.76
Standard deviation	0.685	0.247	0.074

The CTD derived mean sound speed is 1521.0 m/s.

6.3. Distance between two parallel straight-line paths

In addition to knowing how many survey paths are required to achieve a desired accuracy for transponder positioning, knowing the distance between two parallel straight-line paths is an important criterion when determining the accuracy of numerical solutions. Based on Eq. (12), distance D between two parallel survey paths can be derived:

$$D = |(P_{sx2} - P_{sx1})\cos\mu - (P_{sy2} - P_{sy1})\sin\mu|. \tag{34}$$

Table 4
Optimal estimates of the transponder position and the mean sound speed using acoustic and GPS observations collected from two segmented straight-line paths

Straight-line paths	P_{Tx} (m)	P_{Ty} (m)	P_{Tz} (m)	V_a (m/s)
L1, L2	156465.52	2492807.90	−342.96	1520.25
L1, L3	156465.34	2492807.94	−343.17	1521.06
L1, L4	156465.51	2492807.87	−342.96	1520.33
L1, L5	156465.04	2492807.80	−343.12	1521.36
L1, L6	156464.91	2492807.80	−342.82	1520.97
L1, L7	156464.86	2492807.81	−342.92	1521.26
L1, L8	156464.42	2492808.08	−342.29	1520.76
L2, L3	156465.22	2492807.86	−342.79	1520.19
L2, L4	156465.51	2492807.81	−342.69	1519.51
L2, L5	156465.06	2492807.74	−342.75	1520.28
L2, L6	156464.81	2492807.74	−342.53	1520.12
L2, L7	156464.77	2492807.75	−342.55	1520.21
L2, L8	156464.21	2492807.99	−342.15	1520.15
L3, L4	156465.55	2492807.83	−342.95	1520.25
L3, L5	156464.91	2492807.77	−343.13	1521.30
L3, L6	156464.64	2492807.78	−342.88	1520.88
L3, L7	156464.67	2492807.80	−343.02	1521.19
L3, L8	156463.98	2492808.06	−342.55	1520.64
L4, L5	156464.39	2492807.73	−342.91	1520.57
L4, L6	156464.22	2492807.72	−342.75	1520.20
L4, L7	156464.39	2492807.71	−342.84	1520.39
L4, L8	156463.53	2492807.98	−342.56	1519.93
L5, L6	156463.88	2492807.64	−343.21	1521.22
L5, L7	156464.50	2492807.64	−343.29	1521.66
L5, L8	156463.38	2492807.90	−343.16	1521.00
L6, L7	156464.70	2492807.65	−342.98	1521.17
L6, L8	156463.02	2492807.89	−343.22	1520.56
L7, L8	156461.15	2492807.90	−344.81	1521.06
Mean value	156464.50	2492807.82	−342.93	1520.65
Standard deviation	0.927	0.117	0.463	0.524

Mean sound speed in the water column is assumed to be unknown.

Table 5
Optimal estimates of the transponder position and the mean sound speed using acoustic and GPS observations collected from two segmented circular paths

Circular paths	P_{Tx} (m)	P_{Ty} (m)	P_{Tz} (m)	V_a (m/s)
C1, C2	156462.24	2492807.25	−343.13	1522.08
C1, C3	156462.30	2492807.30	−342.62	1520.93
C1, C4	156462.29	2492807.26	−343.21	1522.29
C2, C3	156461.17	2492806.98	−343.64	1523.65
C2, C4	156461.12	2492806.92	−343.53	1523.26
C3, C4	156460.71	2492806.74	−343.16	1522.08
Mean value	156461.64	2492807.08	−343.22	1522.38
Standard deviation	0.718	0.228	0.359	0.967

Mean sound speed in the water column is assumed to be unknown.

Based on Eqs. (33) and (34), the absolute value of the Jacobian determinant for two parallel straight-line paths ($\mu_1 = \mu_2 = \mu$) is

$$|\mathbf{J}_f| = D|(d_1 - d_2)(d_2 - d_3)(d_3 - d_1)|. \tag{35}$$

From Eq. (35), the magnitude of the Jacobian determinant is proportional to the distance D between two straight-line paths. In accordance with the numerical convergence of solutions, a high value of the Jacobian determinant can acquire

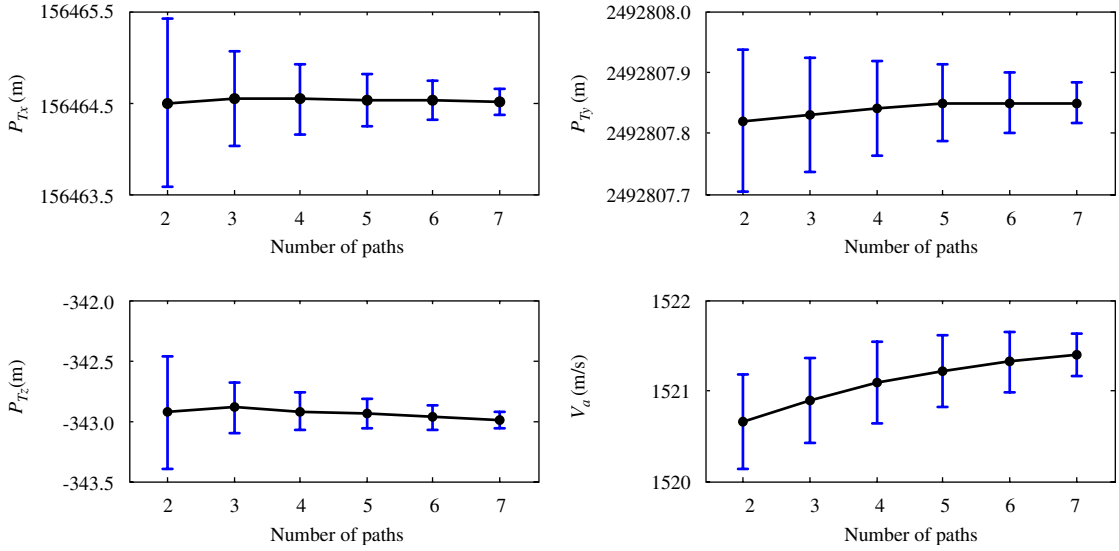

Fig. 5. The values of mean and standard deviation of optimal estimates with the number of segmented paths.

Table 6
Standard deviations of optimal estimates corresponding to the separation distance between two parallel straight-line paths

Paths	Optimal estimates			Distance between paths (m)	Standard deviation (m)		
	P_{Tx} (m)	P_{Ty} (m)	P_{Tz} (m)		$\sigma_{P_{Tx}}$	$\sigma_{P_{Ty}}$	$\sigma_{P_{Tz}}$
L1, L2	156464.97	2492807.95	−342.92	75	1.45	0.14	0.67
L2, L3	156464.98	2492807.92	−342.99				
L3, L4	156465.50	2492807.87	−343.19				
L4, L5	156464.42	2492807.73	−343.06				
L5, L6	156463.82	2492807.63	−343.14				
L6, L7	156464.65	2492807.64	−342.93				
L7, L8	156461.14	2492807.90	−344.80				
L1, L3	156465.34	2492807.93	−343.15	150	0.81	0.12	0.12
L2, L4	156465.14	2492807.89	−343.11				
L3, L5	156464.94	2492807.77	−343.03				
L4, L6	156464.25	2492807.74	−343.03				
L5, L7	156464.40	2492807.61	−343.08				
L6, L8	156463.13	2492807.90	−343.35				
L1, L4	156465.33	2492807.91	−343.15	225	0.73	0.08	0.10
L2, L5	156464.95	2492807.79	−342.99				
L3, L6	156464.62	2492807.78	−342.92				
L4, L7	156464.44	2492807.74	−343.04				
L5, L8	156463.38	2492807.91	−343.16	300	0.61	0.10	0.05
L1, L5	156465.11	2492807.78	−342.99				
L2, L6	156464.75	2492807.80	−342.86				
L3, L7	156464.67	2492807.78	−342.94				
L4, L8	156463.69	2492807.98	−342.93				

additional information for estimation and provide rapid numerical convergence of the iterative process. Thus, we expect that the accuracy of numerical solutions of the optimization problem improves when distance D between two straight-line paths increases.

The eight straight-line paths shown in Fig. 4(a) are roughly evenly spaced with a separation of 75 m. According to the results in Table 2, the standard deviations of those estimates corresponding to the same distance between two straight-line paths are calculated, and the results are shown in Table 6. Apparently, the distance between two straight-line paths is inversely related to the standard deviation in estimating the position of a transponder. This experimental result verifies the

analytical prediction mentioned above that the accuracy of numerical solutions improves when distance D between two straight-line paths increases.

7. Conclusions

This study proposed circular and straight-line survey patterns to collect acoustic and GPS observations for estimating the position of a seafloor transponder. This study proved mathematically, that in the case of circular surveys, observations collected along a circular path can determine the position of a transponder when sound speed is known. When the sound speed profile is unavailable, surveys along at least two circular paths with different radii are needed to determine the position of a transponder and the mean sound speed. This study also proved that in the case of straight-line surveys, observations collected along a straight-line path cannot locate the transponder uniquely even when sound speed is known. A survey along at least two straight-line paths is required to uniquely determine the position of a transponder regardless of whether sound speed is known. Based on experimental results, the position of a seafloor transponder can be accurately estimated using an optimization algorithm to minimize the sum of squares of the differences between observed and predicted slant ranges. Moreover, the mean sound speed of the water column estimated via the optimization approach is in agreement with that derived from CTD measurements. Experimental results also confirm the analytical prediction that increasing the distance between two parallel survey paths improves the accuracy of optimal estimates. With the great uncertainties inherent in GPS measurements and the use of a commercial acoustic transponder not designed for precise ranging, field experiment results demonstrate that the seafloor transponder can be localized using optimization algorithm with an uncertainty of decimeters. We believe that the position of a seafloor transponder can be estimated with an uncertainty at the centimeter-level when the accuracy of GPS and acoustic systems is improved.

Acknowledgments

The authors would like to thank the Asian Pacific Ocean Research Center of National Sun Yat-sen University for financially supporting this research under Contract No. 94C030333. It is also a pleasure to acknowledge with gratitude the financial supports of the National Science Council of Taiwan under Contract No. NSC 94-2611-E-110-009. The assistance of Professors Ming-Chung Fung and Min-Chih Huang of the Department of Systems and Naval Mechatronic Engineering, National Cheng Kung University, is appreciated for kindly providing instrumental support in carrying out the field experiment.

References

Bevis, M., Taylor, F.W., Schutz, B.E., Recy, J., Isacks, B.L., Helu, S., Singh, R., Kendrick, E., Stowell, J., Taylor, B., Calmant, S., 1995. Geodetic observations of very rapid convergence and back-arc extension at the Tonga arc. Nature 374, 249–251.

Caiti, A., Garulli, A., Livide, F., Prattichizzo, D., 2005. Localization of autonomous underwater vehicles by floating acoustic buoys: a set-membership approach. IEEE Journal of Oceanic Engineering 30 (1), 140–152.

Chen, C., Millero, F.J., 1977. Speed of sound in seawater at high pressures. Journal of the Acoustical Society of America 62 (5), 1129–1135.

Hildebrand, F.B., 1976. Advanced Calculus for Applications. Prentice-Hall, Englewood Cliffs, NJ.

Kussat, N.H., Chadwell, C.D., Zimmerman, R., 2005. Absolute positioning of an autonomous underwater vehicle using GPS and acoustic measurements. IEEE Journal of Oceanic Engineering 30 (1), 153–164.

Milne, P.H., 1983. Underwater Acoustic Positioning Systems. Gulf Pub. Co, Huston.

Obana, K., Katao, H., Ando, M., 2000. Seafloor positioning system with GPS-acoustic link for crustal dynamics observation—a preliminary result from experiments in the sea. Earth Planets Space 52, 415–423.

Opderbecke, J., 1997. At-sea Calibration of a USBL Underwater Vehicle Positioning System, vol. 1. IEEE/MTS OCEANS'97, Halifax, NS, Canada, pp. 721–726.

Osada, Y., Fujimoto, H., Miura, S., Sweeney, A., Kanazawa, T., Nakao, S., Sakai, S., Hildebrand, J.A., Chadwell, C.D., 2003. Estimation and correction for the effect of sound velocity variation on GPS/acoustic seafloor positioning: an experiment off Hawaii Island. Earth Planets Space 55, e17–e20.

Osler, J., Beer, J., 2000. Real-time Localization of Multiple Acoustic Transponders Using a Towed Interrogation Transducer, vol. 1. IEEE/MTS OCEANS 2000, Providence, RI, USA, pp. 725–732.

Philips, D., 2003. An evaluation of USBL and SBL acoustic systems and the optimisation of methods of calibration-part 2. The Hydrographic Journal 109, 10–20.

Saab, S.S., Charbachy, D.S., 2000. Differential GPS performance: ground versus geostationary satellite. The Seventh IEEE International Conference on Electronics, Circuits and Systems, ICECS 2000, vol. 1, Jounieh, Lebanon, pp. 357–360.

Shevenell, M.P., 1984. Transponder net self calibration algorithm. OCEANS 16, 60–63.

Shiobara, H., Nakanishi, A., Shimamura, H., Mjelde, R., Kanazawa, T., Eivind, E., 1997. Precise positioning of ocean bottom seismometer by using acoustic transponder and CTD. Marine Geophysical Researchers 19, 199–209.

Spiess, F.N., Chadwell, C.D., Hildebrand, J.A., Young, L.E., Purcell Jr., G.H., Dragert, H., 1998. Precise GPS/acoustic positioning of seafloor reference points for tectonic studies. Physics of the Earth and Planetary Interiors 108, 101–112.

Sweeney, A.D., Chadwell, A.D., Hildebrand, J.A., Spiess, F.N., 2005. Centimeter-level positioning of seafloor acoustic transponders from a deeply-towed interrogator. Marine Geodesy 28, 39–70.

Yamada, T., Ando, M., Tadokoro, K., Sata, K., Okuda, T., Oike, K., 2002. Error evaluation in acoustic positioning of a single transponder for seafloor crustal deformation measurements. Earth Planets Space 54, 871–881.

Yoerger, D.R., Bradley, A.M., Singh, H., Walden, B.B., Cormier, M.-H., Ryan, W.B.F., 2000. Multisensor mapping of the deep seafloor with the autonomous benthic explorer. The 2000 International Symposium on Underwater Technology, Tokyo, Japan, pp. 248–253.